Geol. Mag. **150** (*6*), *2013, pp. 959–974.* © *Cambridge University Press 2013*
doi:10.1017/S0016756812000969

Detrital zircon provenance of the Lower Yangtze foreland basin deposits: constraints on the evolution of the early Palaeozoic Wuyi–Yunkai orogenic belt in South China

HAI-BIN LI*, DONG JIA*†, LONG WU*, YONG ZHANG*, HONG-WEI, YIN*, GUO-QI WEI‡ & BEN-LIANG LI§

*State Key Laboratory for Mineral Deposits Research, Institute of Energy Sciences and Department of Earth Sciences, Nanjing University, Nanjing 210093, China
‡Research Institute of Petroleum Exploration and Development, Petrochina, Langfang Branch, Langfang 065007, China
§Research Institute of Petroleum Exploration and Development, Petrochina, Beijing 100083, China

(*Received* 8 August 2011; *accepted* 1 November 2012; *first published online* 21 March 2013)

Abstract – The Lower Yangtze foreland basin is situated to the northwest of the early Palaeozoic Wuyi–Yunkai orogen in South China. To demonstrate its provenance history and the denudation of the orogen, seven sandstone samples were collected from the upper Ordovician to Silurian strata for U–Pb dating. The zircons show a broad range of ages that can be linked with the ages of specific units in the Wuyi–Yunkai orogen. The zircon spectra in the late Ordovician samples are similar to those in the pre-orogenic strata, suggesting a recycled source. The dominant age population of 880–740 Ma in the early Llandovery samples indicates that the middle Neoproterozoic volcanic rocks were the primary source. A significant age population of 460–425 Ma in the late Llandovery to Wenlock samples reflects the fact that the synorogenic magmatic and metamorphic rocks were exposed to provide detritus. The youngest zircons from the uppermost Silurian strata yield an age of 425 Ma, which approximates the inferred depositional age. This age, together with available biostratigraphic data, indicates that the foreland basin was formed 448–425 Ma ago. We surmise a possible link between the Wuyi–Yunkai orogen and the Appalachian–Caledonian orogen based on the geological constraints and palaeomagnetic data.

Keywords: U–Pb dating, Lower Yangtze foreland basin, Wuyi–Yunkai orogen, South China.

1. Introduction

South China is characterized by a NE–SW-trending orogen, which stretches for *c*. 2000 km and is termed the Wuyi–Yunkai orogen (Fig. 1a; Li *et al*. 2010). Owing to its tectonic significance, systematic studies have been performed on the metamorphism, magmatism and deformation. Precise geochronological data from the associated magmatic and metamorphic rocks indicate that the orogen took place during the period of 460–420 Ma (Wang, Y. J. *et al*. 2007, 2011; Faure *et al*. 2009; Charvet *et al*. 2010; Li *et al*. 2011; Li *et al*. 2010; Liu *et al*. 2010; Wan *et al*. 2010; Yang *et al*. 2010). However, so far little information has been obtained from the synorogenic deposits, which may record the growth and denudation of the orogen.

The upper Ordovician to Silurian strata are thick and widespread in the Yangtze region. The strata consist of sandstone, siltstone and mudstone, which are distinct from the underlying carbonate sediments and are overlain disconformably by the upper Devonian rocks. These rocks are interpreted to have been deposited in a foreland basin related to the Wuyi–Yunkai orogen (Liu & Xu, 1994; Chen *et al*. 1997; Li *et al*. 2010). Thus, the provenance, age, thickness and distribution of these strata record the development of the foreland basin and the evolution of the Wuyi–Yunkai orogen. The foreland basin deposits have been assumed to be derived from the Wuyi–Yunkai orogen, largely on the basis of palaeocurrent data and lithofacies analyses (Liu & Xu, 1994; Rong *et al*. 2003; Chen *et al*. 2004). It is still unclear which units of the orogen the detritus was derived from. Another problem is that the age of the upper unit of the Silurian strata is not well constrained, because the fossils are rather scarce in the unit. It has been loosely assigned to the Wenlock (Chen *et al*. 1988) or Telychian (Rong *et al*. 2003).

In this study, we present U–Pb geochronological data from detrital zircons from the late Ordovician to Silurian sandstone samples taken across the Lower Yangtze foreland basin (Fig. 1b). Dating of detrital zircons is a powerful tool for constraining sedimentary provenance and basin analysis, because it can provide important information regarding the age and nature of source rocks and determine the maximum age of a stratigraphic succession (e.g. Cawood *et al*. 1999, 2007). The new data provide significant insights into the depositional age and the provenance history of the

† Author for correspondence: djia@nju.edu.cn

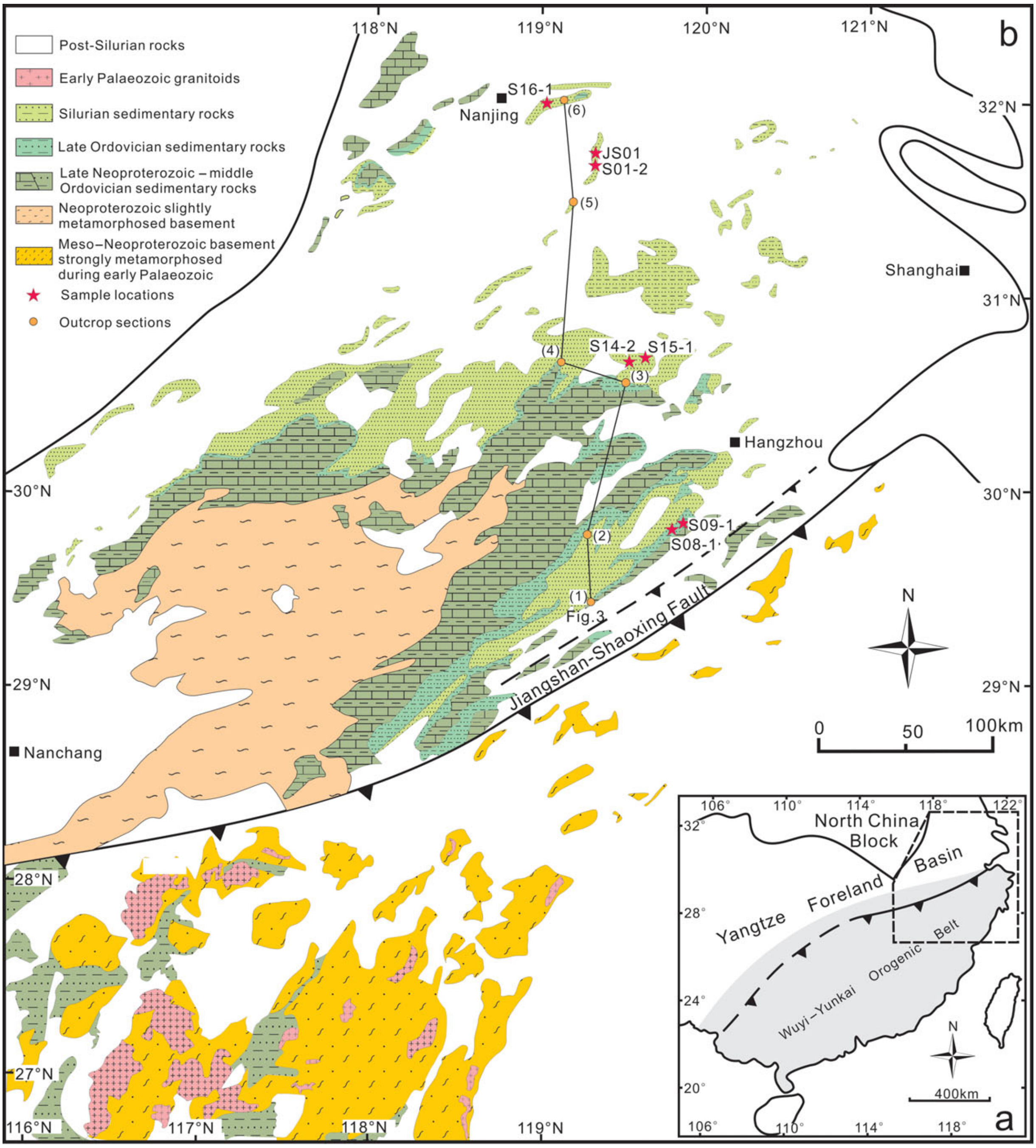

Figure 1. (a) Tectonic framework of South China. (b) Geological map of the Lower Yangtze foreland basin and the adjacent Wuyi–Yunkai orogenic belt.

foreland basin as well as the growth and exhumation of the Wuyi–Yunkai orogen.

2. Geological setting

The South China block consists of the Yangtze block to the northwest and the Cathaysia block to the southeast. The present northeastern boundary of the two blocks is the Jiangshan–Shaoxing fault, while the other parts of the boundary are not clear owing to poor exposure and younger tectonic modifications (Li *et al*. 2010). The two blocks were amalgamated during *c*. 900–880 Ma (e.g. Li, W. X. *et al*. 2008) or *c*. 800 Ma (Zhao & Cawood, 1999; Zhou *et al*. 2002; Wang *et al*. 2006). Following the amalgamation, continental rifting occurred in the South China block and produced thick volcanic and volcaniclastic deposits (Li *et al*. 1999; Wang & Li, 2003; Zheng *et al*. 2008). The rifting failed (Charvet *et al*. 2010; Li *et al*. 2010) or evolved into a small ocean (Liu & Xu, 1994) in the middle Neoproterozoic. During the late Neoproterozoic, the rifting ceased and was followed by thermal subsidence over the region (Wang & Li, 2003). Three distinct depositional settings developed in the South China block, namely the Yangtze platform, slope and basin. The platform–slope deposits are represented

https://doi.org/10.1017/S0016756812000969 Published online by Cambridge University Press

by carbonate, and the basinal sediments are composed of rhythmically interbedded sandstone, siltstone and mudstone. These depositional environments persisted until the late Ordovician (Chen *et al.* 2004; Chen, Zhou & Fan, 2010). Some authors (Zhang, Liou & Coleman, 1984; Liu & Xu, 1994; Chen *et al.* 1997; Jiang, Kennedy & Christie-Blick, 2003; Jiang, Sohl & Christie-Blick, 2003; Zhou *et al.* 2004; Bradley, 2008) inferred that the platform–slope–basin system was deposited in a passive margin setting based on the platform scale and comparatively simple physical stratigraphic and facies architecture with no evidence of tectonic activity (Jiang, Sohl & Christie-Blick, 2003). However, there is as yet no direct evidence for an ocean adjacent to the inferred passive margin (Ren, 1991; Charvet *et al.* 2010; Li *et al.* 2010), while the provenance studies of the lower Palaeozoic basinal sediments indicate that they accumulated in an intracontinental basin (Wang *et al.* 2010). Deposition in the basin was terminated by the orogeny during the late Ordovician to Silurian, and in front of the northeastern Wuyi–Yunkai orogen a foreland basin was formed in the Yangtze region.

The Wuyi–Yunkai orogen includes Palaeoproterozoic to lower Neoproterozoic high-grade metamorphic rocks, upper Neoproterozoic – lower Palaeozoic low-grade metamorphic sedimentary rocks, and lower Palaeozoic migmatites and granitoids (e.g. Faure *et al.* 2009; Charvet *et al.* 2010; Shu *et al.* 2011). The high-grade metamorphic rocks include gneiss, micaschist, quartzite, marble, amphibolite and granulite, which were generally considered to be the Proterozoic basement (Zhao & Cawood, 1999). However, recent geochronological results reveal that some of these rocks have protolith ages of 830–700 Ma and were metamorphosed at approximately 460–440 Ma (Wan *et al.* 2007; Charvet *et al.* 2010; Li *et al.* 2011; Li *et al.* 2010). The upper Neoproterozoic – lower Palaeozoic rocks consist of phyllite, slate, meta-shale and meta-sandstone with a thickness of up to 7–8 km. Those rocks were metamorphosed in the sub-greenschist to lower-greenschist facies, intensely folded and unconformably overlain by the Devonian sandstones. The lower Palaeozoic migmatites and granitoids are widespread, and reliable geochronological data indicate that they were formed at 460–420 Ma (Wang, Y. J. *et al.* 2007; Charvet *et al.* 2010; Li *et al.* 2010; Wan *et al.* 2010; Xu *et al.* 2011). The Jiangshan–Shaoxing fault was most likely reactivated and acted as a significant fault during the orogeny, because the upper Neoproterozoic–Ordovician strata north of the fault were not metamorphosed and the structures on both sides of the fault are very different (e.g. Charvet *et al.* 1996, 2010; Faure *et al.* 2009). Systematic studies in the central-northern part of the Wuyi–Yunkai orogen reveal that the orogen has a doubly vergent fan structure, and north of the Jiangshan–Shaoxing fault, the structures are characterized by N-directed thin-skinned deformation, whereas south of the fault, the structures are represented by S-directed thin-skinned and thick-skinned deformation as well as top-to-the-S shearing in the orogen proper and on its southern border (Charvet *et al.* 2010). The fault was probably active again during the Permian–Jurassic deformation (Charvet *et al.* 1996; Li *et al.* 2010). The Lower Yangtze foreland basin was formed in response to N- or NW-verging thrusting of the Wuyi–Yunkai orogen. It is uncertain whether or not there exists a foreland basin on the other side of the orogen, because no synorogenic sedimentary rocks have been discovered.

The Yangtze block is generally considered to have an Archaean to early Neoproterozoic basement. The oldest rocks are composed of Archaean to Palaeoproterozoic migmatites and gneisses (e.g. Qiu *et al.* 2000). The Mesoproterozoic to early Neoproterozoic basement comprises a sequence of metasandstone, slate and phyllite. This sequence was folded during the amalgamation of the Yangtze block with the Cathaysia block, and unconformably overlain by middle to upper Neoproterozoic rift-related volcanic and sedimentary rocks (Charvet *et al.* 1996; Wang & Li, 2003; Wang, X. L. *et al.* 2007). The upper Neoproterozoic to middle Ordovician strata consist of dolomites, limestones and shales, which were deposited in a SE-dipping platform-to-slope setting (e.g. Liu & Xu, 1994; Vernhet *et al.* 2006; Chen, Zhou & Fan, 2010). The strata near the Jianshan–Shaoxing fault were involved in the deformation during the Wuyi–Yunkai orogeny (Charvet *et al.* 2010; Li *et al.* 2010). The upper Ordovician to Silurian strata consists of siliciclastic sediments and are well preserved in the Lower Yangtze foreland basin. Detailed biostratigraphic correlations have been established (Mu *et al.* 1986; Rong & Chen, 1987; Chen *et al.* 1988, 2000, 2004; Chen & Rong, 1996; Rong *et al.* 2003, 2010), which facilitate this study.

3. Foreland basin stratigraphy

The Lower Yangtze foreland basin began to form in the late Ordovician and continued into the Wenlock (Liu & Xu, 1994; Rong *et al.* 2003). The initial development of the foreland basin is indicated by the significant changes in deposition rate, biofacies and palaeogeography in the late Katian (Chen *et al.* 1997; Rong *et al.* 2010). The geographic distribution and general lithologic characteristics of the foreland basin strata are described below.

The upper Katian to Hirnantian stratigraphy of the Lower Yangtze basin has been comprehensively studied (Chen *et al.* 1988, 2000, 2004, 2010; Chen, Zhou & Fan, 2010; Rong *et al.* 2010), and four graptolite zones have been established for high-resolution stratigraphic correlation (Fig. 2). The strata are composed of closely spaced rhythmic sandstone and mudstone and form a southeastward-thickening wedge. The thickness reaches 2500 m in the front of the orogenic belt and decreases towards the northwest (Fig. 3). In the Nanjing area, the strata are dominated by *c.* 10 m thick black shale, which thickens up to 100 m to the north of the

https://doi.org/10.1017/S0016756812000969 Published online by Cambridge University Press

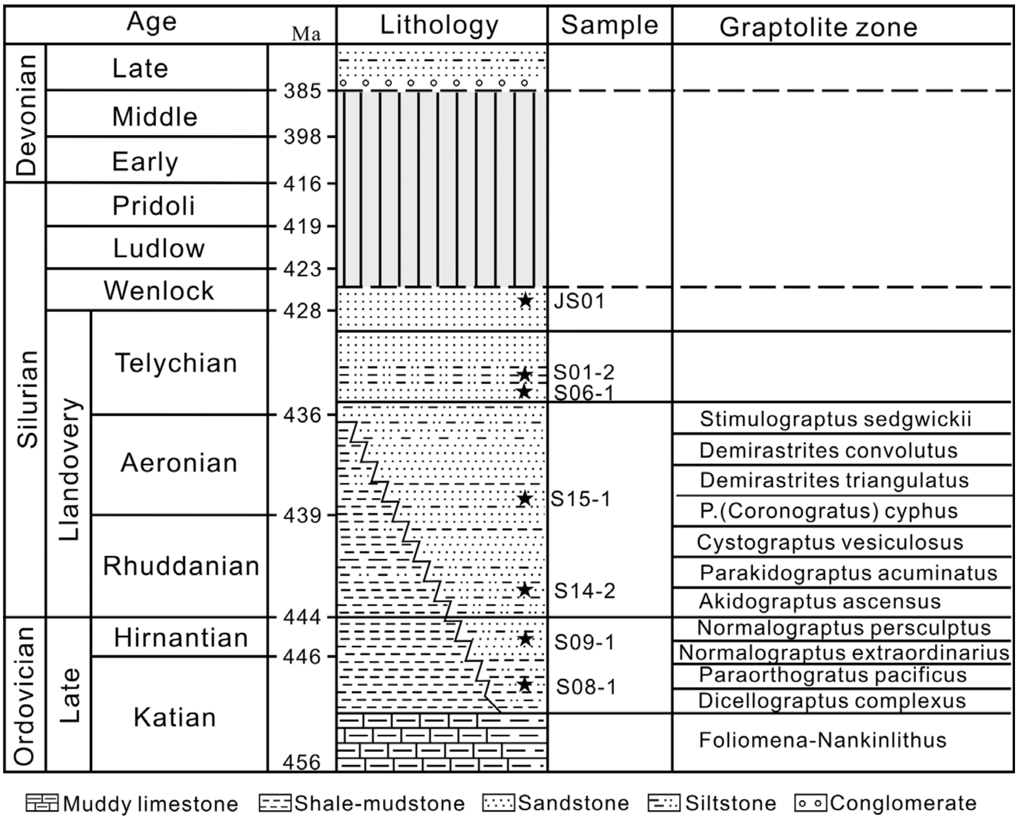

Figure 2. Stratigraphy of the Lower Yangtze foreland basin (modified after Mu *et al*. 1986, Chen *et al*. 2000 and Rong *et al*. 2003) showing approximate position of analysed samples.

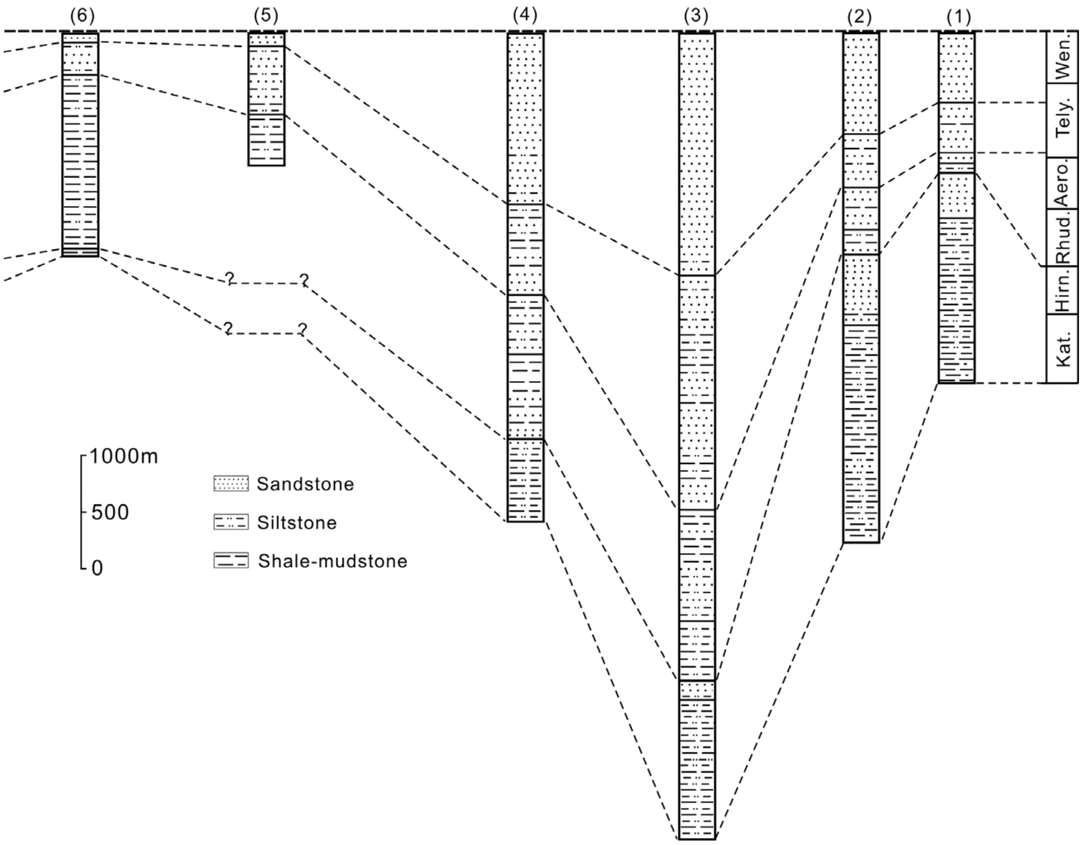

Figure 3. Regional composite stratigraphic sections of upper Ordovician to Silurian rocks considered in this study. Sources of data for sections 1, 2, 3 – ZBGMR (1965, 1989); 4 – ABGMR (1997); 5, 6 – JBGMR (1984).

https://doi.org/10.1017/S0016756812000969 Published online by Cambridge University Press

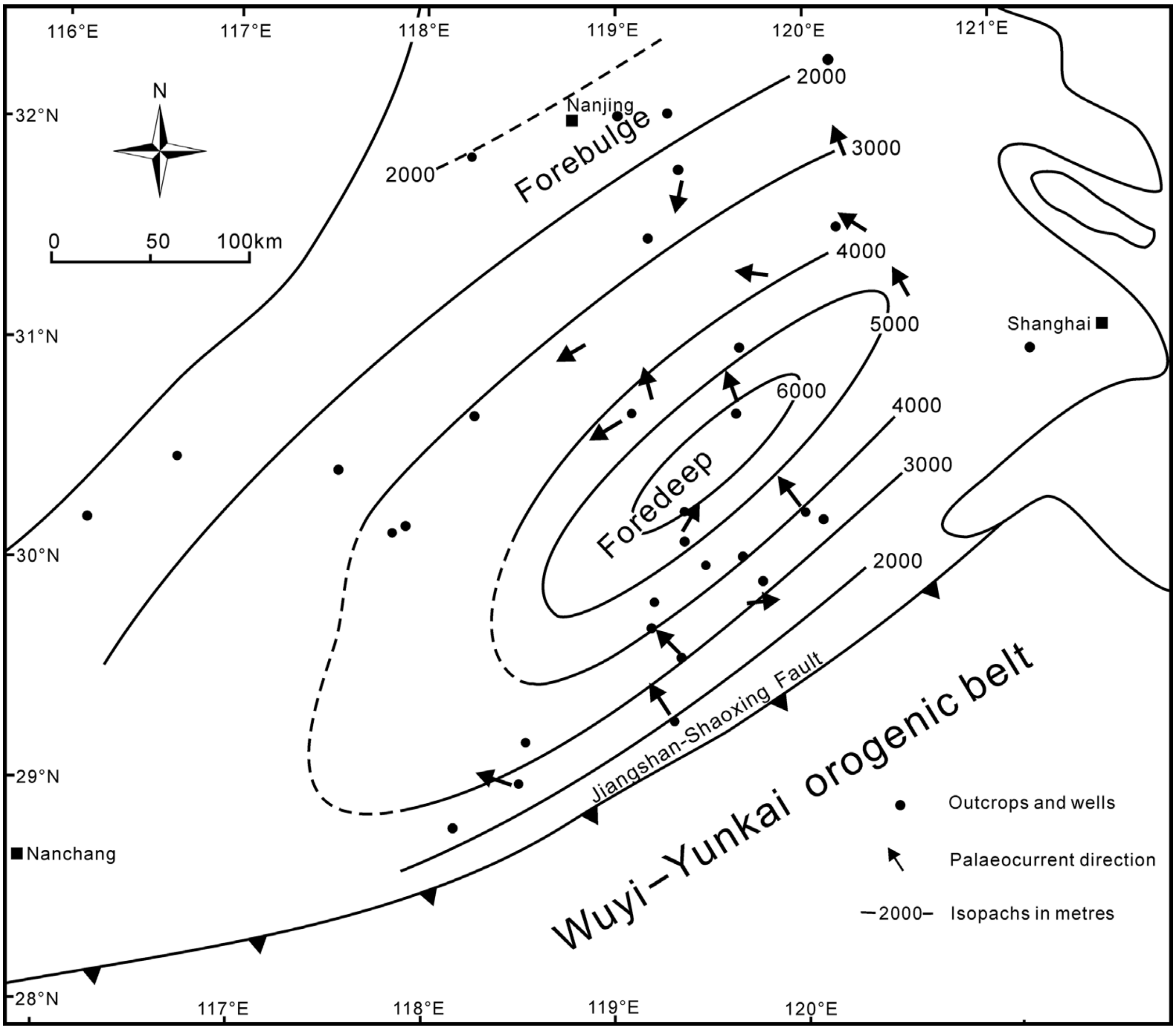

Figure 4. Isopachs map of the upper Ordovician to Silurian strata. Solid arrows represent mean palaeocurrent directions (modified after Hongbo Lu, unpub. Masters thesis, Nanjing Univ., 1985; Xia & Lu, 1990). Contours are in metres and the data sources are ABGMR (1997), JBGMR (1984) and ZBGMR (1965, 1989).

study area (Chen *et al.* 1988). The trend in thickness implies that there is a possible flexural uplift along the Nanjing area. Lithofacies and palaeocurrent data indicate an overall southeastern source (Hongbo Lu, unpub. Masters thesis, Nanjing Univ., 1985; Liu & Xu, 1994).

The Silurian strata conformably overlie the upper Ordovician strata and are generally subdivided into three units based on lithostratigraphy and biostratigraphy. The lower unit is composed of shale, mudstone and sandstone with lithologic variations across the basin. The northern part of the basin is dominated by black to yellow shale and mudstone, and reaches a maximum thickness of *c.* 1500 m (Fig. 3). Abundant graptolite fossils retrieved from the shale and mudstone define a Rhuddanian–Aeronian age of deposition (Fig. 2). Towards the orogenic belt, the unit thickens and grades into grey-green siltstone and fine sandstone with fewer fossils. The middle unit, which is generally interpreted as being Telychian in age, consists of quartz sandstone and silty shale with small amounts of brachiopods, bivalves, trilobites, chitinozoa and conodonts, but no graptolites (Rong *et al.* 2003). The thickness ranges from 200 m to *c.* 2000 m towards the orogenic belt. Cross-bedding and ripple marks are common in the strata, which suggests a shallow marine environment. The upper unit is composed of grey and red quartz sandstone interbedded with siltstone that were interpreted as shallow marine or even non-marine deposits (Mu *et al.* 1986; Chen & Rong, 1996). The fossils are rather scarce in this unit, and the unit is assigned to the late Telychian (Rong *et al.* 2003) or Wenlock (Mu *et al.* 1986; Chen *et al.* 1988) according to limited fossils and regional lithostratigraphic correlations. The thickness reaches up to 2100 m in the southern part of the basin and decreases northwards to *c.* 20 m in the Nanjing area, and then increases up to 170 m to the north (JBGMR, 1984). Foresets and flute casts show dominant palaeocurrent directions towards the NW and WSW (Xia & Lu, 1990).

In order to depict the overall configuration of the foreland basin, an isopach map (Fig. 4) is constructed from published thickness data (ZBGMR, 1965, 1989;

https://doi.org/10.1017/S0016756812000969 Published online by Cambridge University Press

JBGMR, 1984; ABGMR, 1997). Owing to limited postdepositional burial history, the thickness values are not corrected for the effect of compaction. The strata have a maximum thickness of up to 6 km in the northwestern Hangzhou area, and thin regionally towards both the southeast and northwest to *c.* 2 km. Several wells to the north of the study area indicate that the strata increase in thickness (JBGMR, 1984). Stratigraphic thicknesses are not constrained in the eastern section of the basin owing to the lack of outcrops and well data. The regional thickness trend of the strata roughly reflects the position of the foredeep, forebulge and backbulge depozones.

4. Provenance analysis

4.a. Methods

Zircons were extracted from seven samples with standard heavy liquid and magnetic separation methods. Once separated, the zircon grains were mounted in epoxy resin and then polished to expose their interiors. Afterwards, the zircons were examined with transmitted and reflected light photomicrography as well as backscattered electron/cathodoluminescence (BSE/CL) images to identify their internal structures and select spots for analysis.

U–Pb zircon dating was performed using an Agilent 7500 inductively coupled plasma mass spectrometer (ICP-MS), coupled to a New Wave Research 213 nm microprobe in the State Key Laboratory for Mineral Deposits Research at Nanjing University. The analyses were carried out using a beam of 21–35 μm with a laser repetition rate of 5 Hz. Samples were analysed in separate runs and each run consisted of about ten unknown analyses bracketed by four analyses of the GJ zircon standard (608 Ma; Jackson *et al.* 2004). A well-characterized Mud Tank zircon was analysed in each run to control instrument stability and reproducibility. Each analysis was 120 s in duration, with gas background measurements being taken over the first 40 s before initiation of ablation. U–Pb ages were calculated from the raw signal data using the online software package Glitter 4.4, an in-house online data reduction program. The detailed analytical procedure and its precision and accuracy are described by Jackson *et al.* (2004). As measurements of the ^{204}Pb isotope cannot be acquired with this approach, common Pb correction was carried out with the method proposed by Andersen (2002). Those analyses with more than 10 % discordance or 10 % reverse discordance are excluded from further consideration. For grains older than 900 Ma, ^{207}Pb–^{206} Pb age was used, and ^{206}Pb–^{238}U age was used for younger grains.

4.b. Results

A total of 564 usable U–Pb analyses were obtained from the seven samples. The results are plotted on concordia diagrams and age-probability plots. The analytical data are presented in Table S1 in the online Supplementary Material at http://journals.cambridge.org/geo.

Sample S08-1 was collected from the upper Katian sandstone on the southern margin of the basin. Most of the zircons are sub-rounded to sub-angular (Fig. 5a, b). A total of 124 grains were analysed, but only yielded 65 concordant or nearly concordant ages (Fig. 6). The zircon ages span a range from 2670 to 723 Ma, and the largest population is within the 860–740 Ma range with peaks at 805 Ma and 858 Ma (Fig. 7). The other ages scattered around 1143 Ma, 1952 Ma and 2434 Ma.

Sample S09-1 was collected from the Hirnantian outcrops adjacent to S08–1. The zircons from this sample are typically sub-rounded (Fig. 5c, d). Analysis of 96 grains yielded 85 usable ages (Fig. 6). The ages range from 2831 to 526 Ma, with remarkable peaks at 790 Ma, 1027 Ma and 1799 Ma (Fig. 7).

Sample S14–2 was collected from the Rhuddanian grey sandstones in the southern part of the study area, and the zircons are sub-rounded to sub-angular (Fig. 5e, f). A total of 84 grains were analysed and most of them are concordant (Fig. 6). The age spectrum is dominated by a peak at *c.* 860–740 Ma, with small peaks at 2480 Ma, 2004 Ma and 1764 Ma (Fig. 7).

Sample S15–1 was collected from the Aeronian sandstones. Most of the zircons are sub-rounded to sub-angular (Fig. 5g, h). Analysis of 108 grains yielded 88 usable ages (Fig. 6), which span a range from 2736 to 439 Ma. The largest population of zircons is within the 880–750 Ma range, with additional peaks at 445 Ma, 1638 Ma, 1768 Ma and 2450 Ma (Fig. 7).

Samples S01–2 and S16–1 were collected from the Telychian sandstones in the northern part of study area. Most of the zircons are sub-rounded to sub-angular (Fig. 5i–l). A total of 177 grains were analysed from the two samples and yielded 168 usable ages (Fig. 6). The age spectra of the two samples are roughly similar and have been plotted together in the cumulative probability diagrams. The zircon age distribution has a broad range from 433 to 3468 Ma, with four distinct peaks at 447 Ma, 835 Ma, 1000 Ma and 2500 Ma, and a small peak at 2000 Ma (Fig. 7).

Sample JS01 was collected from the upper unit of Silurian strata in the middle part of the study area. The majority of the zircons are sub-rounded to sub-angular (Fig. 5m–p). Analysis of 108 grains yielded 103 concordant or nearly concordant ages (Fig. 6). The ages range from 3123 to 425 Ma, with distinct peaks at around 425 Ma, 840 Ma and 2458 Ma (Fig. 7). There are also minor age populations at 1037 Ma and 2016 Ma. Three grains yield an age of 425 Ma, which provides a maximum depositional age for the unit.

5. Discussion

5.a. Sediment source

Integration of U–Pb zircon age data from the seven analysed samples mainly falls into four groups: (1)

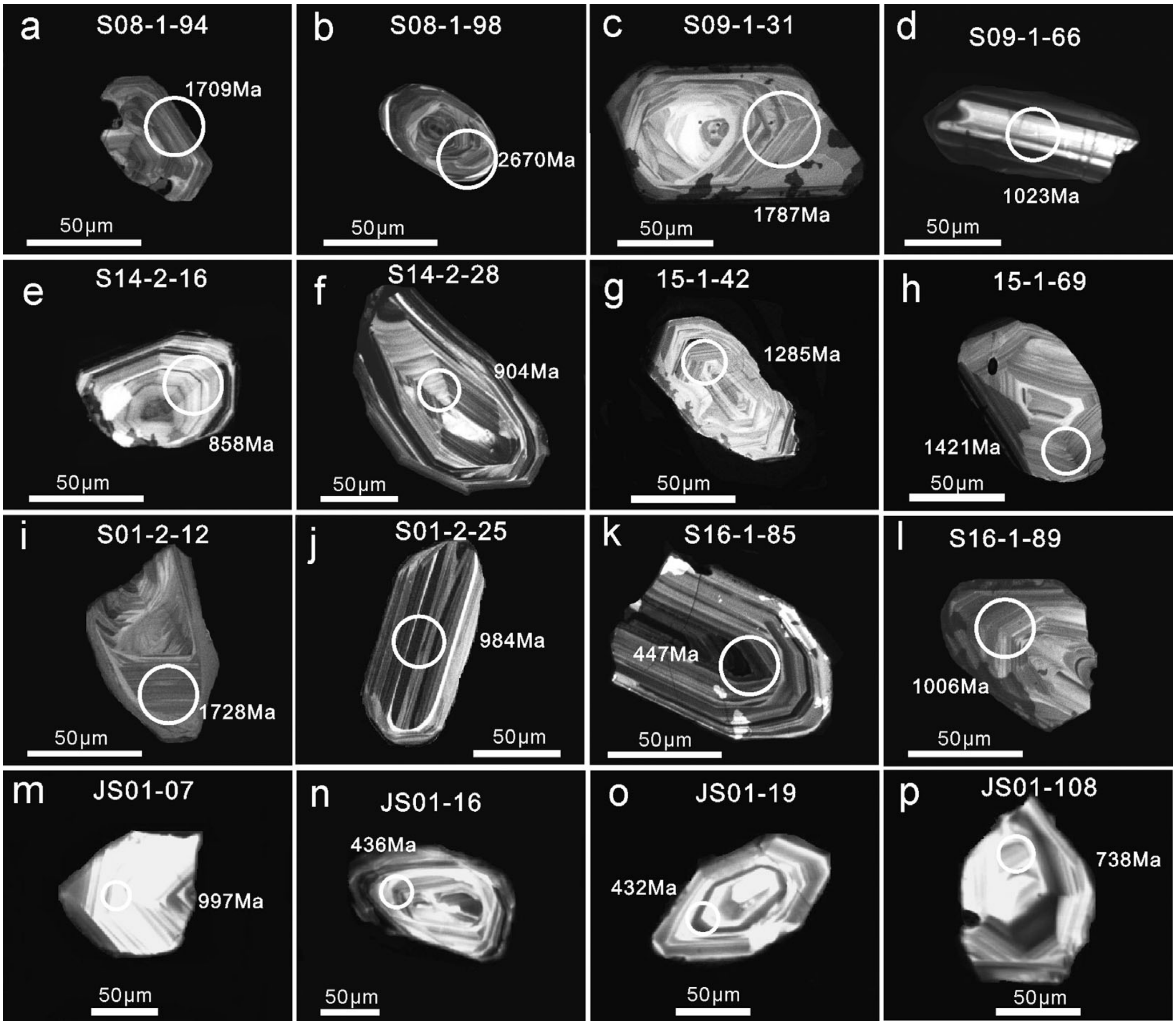

Figure 5. Cathodoluminescence images of representative detrital zircons, showing morphology and internal structure. Circles with ages indicate the laser ablation ICP-MS U–Pb dating spots.

Neoarchaean to Palaeoproterozoic zircons ranging in age from 2840 to 1600 Ma, with peaks at 2500–2400 Ma and 2000–1700 Ma; (2) late Mesoproterozoic to early Neoproterozoic zircons ranging in age from 1200 to 900 Ma, with a pronounced peak at *c.* 1000 Ma; (3) middle Neoproterozoic zircons with ages between 880 and 740 Ma; and (4) early Palaeozoic zircons having ages of 460–425 Ma. The relative proportions of these four age components vary among samples. Neoarchaean to Palaeoproterozoic and middle Neoproterozoic zircons are present in all samples. The zircons with ages of 1200–900 Ma are minor in the samples S14–2 and S15–1 from the Rhuddanian to Aeronian formations. The early Palaeozoic synorogenic zircons are only observed in Silurian samples. The age groupings are similar, and can be linked with the age of specific units in the Wuyi–Yunkai orogen.

Neoarchaean to Palaeoproterozoic source rocks are scarce in South China (Fig. 8). New geochronological data indicate that most of the inferred Palaeoproterozoic and Mesoproterozoic basement rocks in the Cathaysia block were formed in the Neoproterozoic or even later (Wan *et al.* 2007; Yu *et al.* 2009). Only a few Palaeoproterozoic granites and metamorphic rocks have been found in the northeastern part of the Wuyi–Yunkai orogen, which were formed between 1888–1832 Ma (Liu *et al.* 2009; Yu *et al.* 2009) and 1781–1766 Ma (Li *et al.* 2010). These rocks are the likely source for the Palaeoproterozoic zircons, consistent with the basement-involved deformation from the structural and metamorphic studies (Charvet *et al.* 2010; Li *et al.* 2010). Nevertheless, most of the Neoarchaean to Palaeoproterozoic zircons could be recycled from the Neoproterozoic to Ordovician metasedimentary rocks in the Wuyi–Yunkai orogen, as all the age components have been identified in these pre-orogenic sedimentary rocks (Wang, Y. J. *et al.* 2007, 2010; Yu *et al.* 2008; Wu *et al.* 2010; Yao, Shu & Santosh, 2011).

The age population between 1200 and 900 Ma corresponds to the age of the Grenville orogeny. A small number of Grenville-age magmatic and

https://doi.org/10.1017/S0016756812000969 Published online by Cambridge University Press

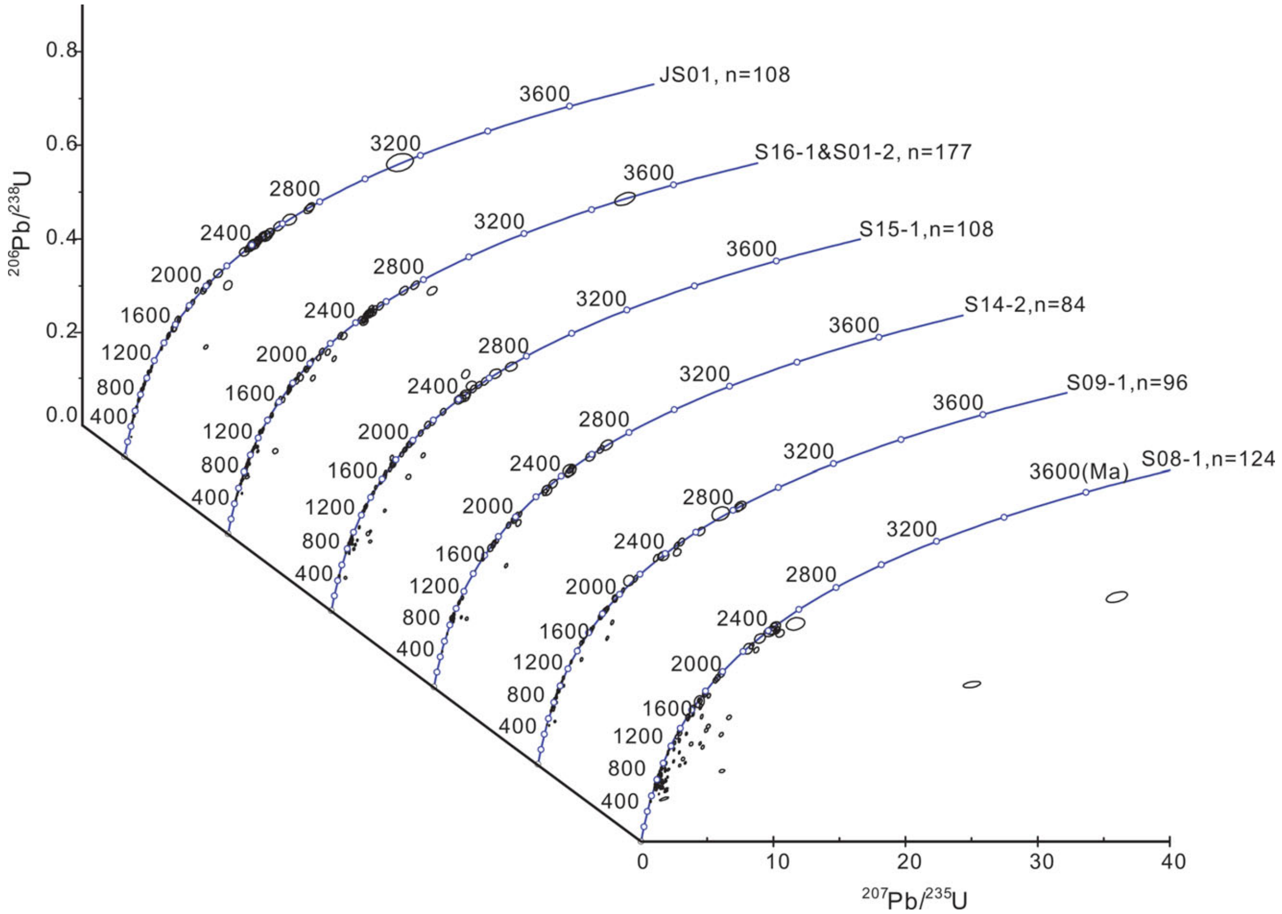

Figure 6. (Colour online) Concordia diagram of dated samples. The name of the individual sample and the number of analysed zircons in the study can be noted next to the concordia curve.

high-grade metamorphic rocks have been found along the western and southeastern margins of the Yangtze (Li *et al*. 1994, 2002; Ye *et al*. 2007), and they are the potential source rocks for the zircons within this age range. Alternatively, these zircons may possibly be predominantly derived from the recycled pre-orogenic sedimentary rocks, which are thick and contain abundant detrital zircons clustered at *c*. 1000 Ma (Yu *et al*. 2008; Wang *et al*. 2010; Wu *et al*. 2010; Yao, Shu & Santosh, 2011). This interpretation is consistent with the fact that the upper Neoproterozoic to Ordovician sedimentary rocks were folded and overlain unconformably by the Devonian strata.

The 880 to 740 Ma population correlates well with the Neoproterozoic magmatic events in the South China block (Fig. 8). Three models have been proposed to interpret the generation of the Neoproterozoic magmas: plume-rift (Li *et al*. 2003), slab-arc (Wang *et al*. 2004) and plate-rift (Zheng *et al*. 2008). Geochronological studies show that the magmatic activity mainly occurred during the periods of *c*. 830–795 Ma and 780–745 Ma (Li *et al*. 2003; Li, X. H. *et al*. 2008; Li, Li & Li, 2005; Wang *et al*. 2006; Zheng *et al*. 2008; Shu *et al*. 2011), and the resulting volcanic and volcaniclastic rocks constitute an original source for the middle Neoproterozoic detritus. Besides, a number of inherited and detrital zircons within this age range have also been found in the upper Neoproterozoic to Ordovician metasedimentary rocks in the Wuyi–Yunkai orogen (Wan *et al*. 2007; Wang *et al*. 2010). These rocks could provide additional detritus.

The early Palaeozoic age group (460–425 Ma) in the detrital zircons falls into the age range of the magmatic and metamorphic rocks formed during the Wuyi–Yunkai orogeny. These rocks provide the only likely source for the early Palaeozoic grains. Most of the zircons show clear oscillatory zoning and high Th/U (Table S1 online Supplementary Material at http://journals.cambridge.org/geo), reflecting their magmatic origin. The presence of these zircons indicates that the synorogenic rocks have been exhumed to supply detritus, which is consistent with the fact that several early Palaeozoic granitic rocks are overlain by Devonian strata (e.g. Xu *et al*. 1960).

5.b. Constraints on the foreland basin development and the orogen evolution

The zircon ages from the upper Ordovician and Silurian strata reveal that the Wuyi–Yunkai orogen is the primary source for the Lower Yangtze foreland basin fills.

Moreover, the temporal trends in zircon age patterns and the youngest zircon ages can also provide new implications for the depositional history of the

https://doi.org/10.1017/S0016756812000969 Published online by Cambridge University Press

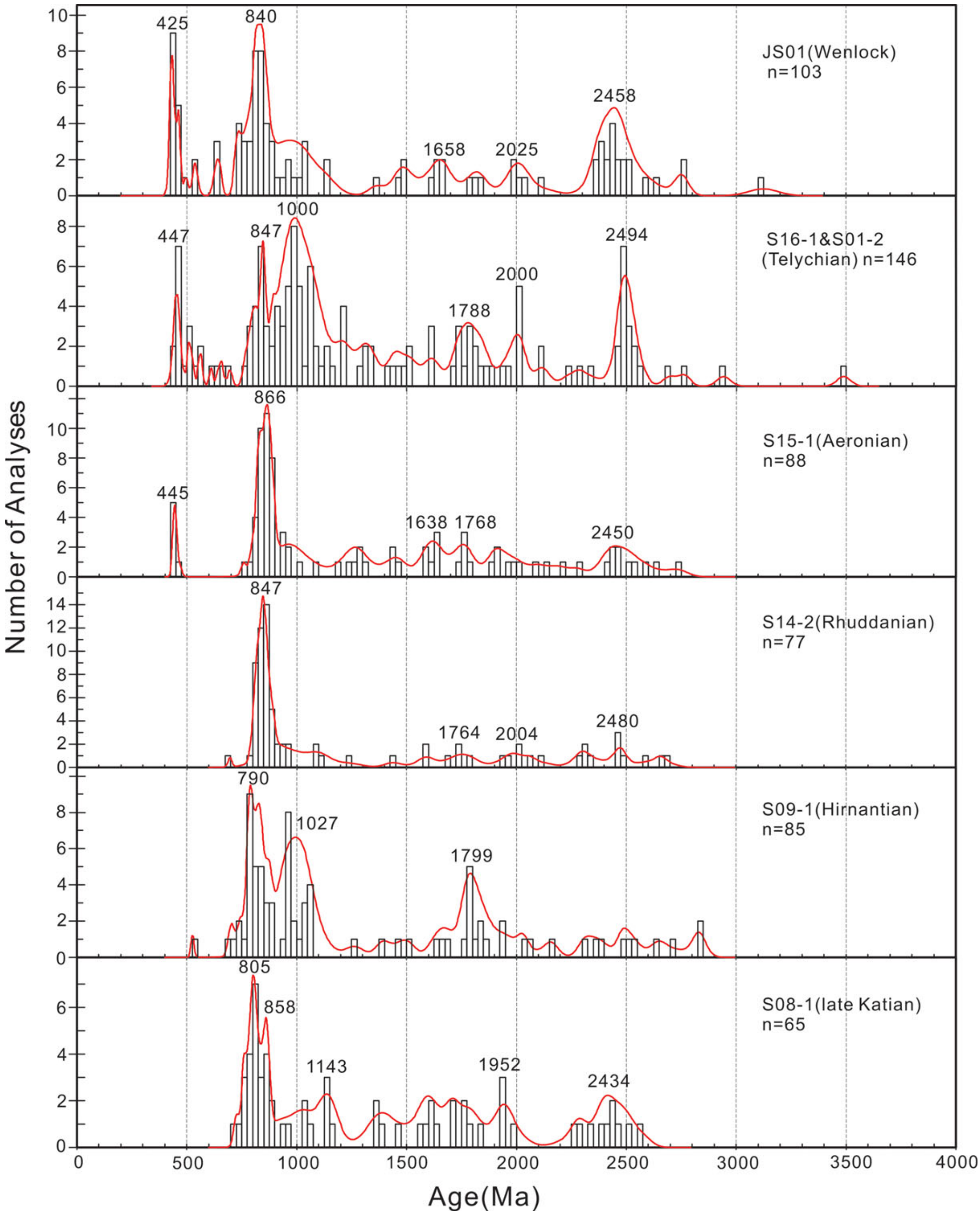

Figure 7. (Colour online) Combined histogram and probability density diagram for 90–110 % concordant analyses. The bin width is 25 Ma. ^{207}Pb–^{206}Pb ages are used for zircons older than 900 Ma.

basin and the unroofing process of the Wuyi–Yunkai orogen. Integration of the new provenance data and sedimentologic and stratigraphic features allows us to correlate the growth and denudation of the Wuyi orogen belt with the foreland basin development, and propose the following evolution model.

Following the rifting during the middle to late Neoproterozoic, a platform–slope–basin environment (Fig. 9a) developed across the South China block (e.g. Liu & Xu, 1994; Vernhet *et al*. 2006; Chen, Zhou & Fan, 2010). In the early Katian, a rapid increase in depositional rate occurred in the basin setting, which may reflect the initial deformation of the Wuyi–Yunkai orogeny (Chen *et al*. 2010).

During the late Katian, great changes in lithofacies and palaeogeography took place in the study area (Chen *et al*. 2004; Rong *et al*. 2010), and the carbonate production was impeded by the progradation of mud, silt and fine sandstone, which marked the initiation of the Lower Yangtze foreland basin. The detritus

https://doi.org/10.1017/S0016756812000969 Published online by Cambridge University Press

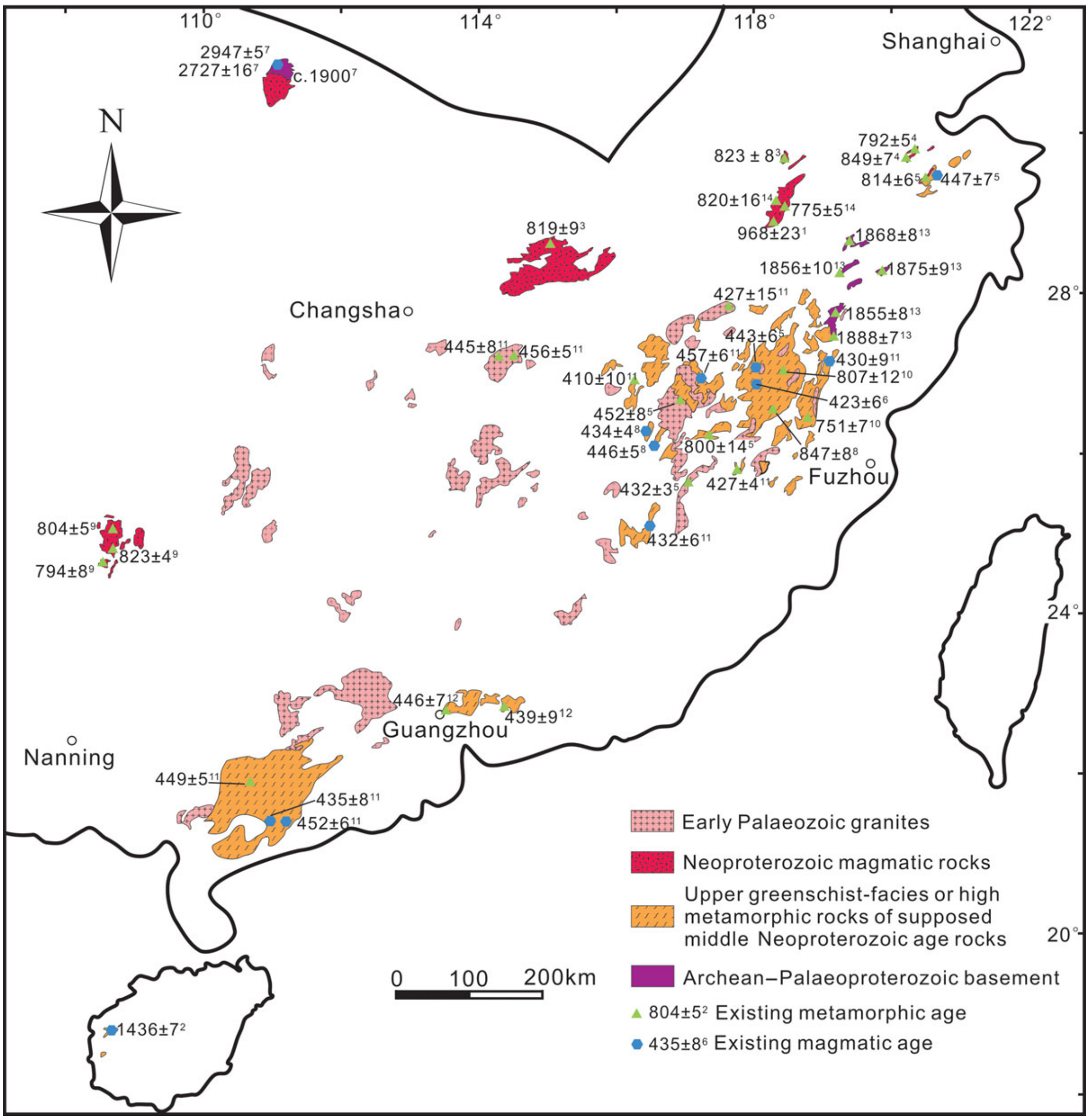

Figure 8. Distribution of pre-Devonian magmatic rocks and high-grade metamorphic rocks in South China. Sources for existing ages as shown in the figure are: 1 – Li *et al*. (1994); 2 – Li *et al*. (2002); 3 – Li *et al*. (2003); 4 – Li, X. H. *et al*. (2008); 5 – Li *et al*. (2010); 6 – Li *et al*. (2011); 7 – Qiu *et al*. (2000); 8 – Shu *et al*. (2011); 9 – Wang *et al*. (2006); 10 – Wan *et al*. (2007); 11 – Wang *et al*. (2011); 12 – Yang *et al*. (2010); 13 – Yu *et al*. (2009); 14 – Zheng *et al*. (2008).

formed a thick clastic wedge in the southern part of the basin (Fig. 9b). The two samples from the strata have multiple peaks and lack early Palaeozoic zircons. The age distributions are similar to those of the late Neoproterozoic to middle Ordovician metasedimentary strata in the Wuyi–Yunkai orogen (Wu *et al*. 2010; Wang *et al*. 2010; Yao, Shu & Santosh, 2011), implying that the late Ordovician detritus was predominantly derived from the recycled rocks. On the other hand, the metasedimentary strata are ideal candidates for source rocks because they are very thick, folded and unconformably overlain by Devonian strata in most parts of the orogen. The pressure–temperature–time history of the metamorphic rocks also reveals a possibly rapid uplift in the northeastern part of the Wuyi–Yunkai orogen during this interval (Li *et al*. 2010). However, first-cycle detritus from the Precambrian source area is also possible. The absence of the early Palaeozoic population suggests that contemporaneous zircon-bearing magmatic rocks were quite likely not yet exposed and exhumed.

During Rhuddanian to Aeronian (early to middle Llandovery) times, the thrusting continued and caused massive subsidence of the foreland basin (Fig. 9c). The two samples from the Rhuddanian and Aeronian (early Silurian) strata are dominated by middle Neoproterozoic zircons. This indicates that large volumes of the sediments were shed from the middle Neoproterozoic volcanic rocks, which were likely uplifted by the S-verging thick-skinned deformation (Charvet *et al*. 2010). The lack of Grenville-age zircon detritus in the strata rules out the pre-orogenic rocks as a significant

https://doi.org/10.1017/S0016756812000969 Published online by Cambridge University Press

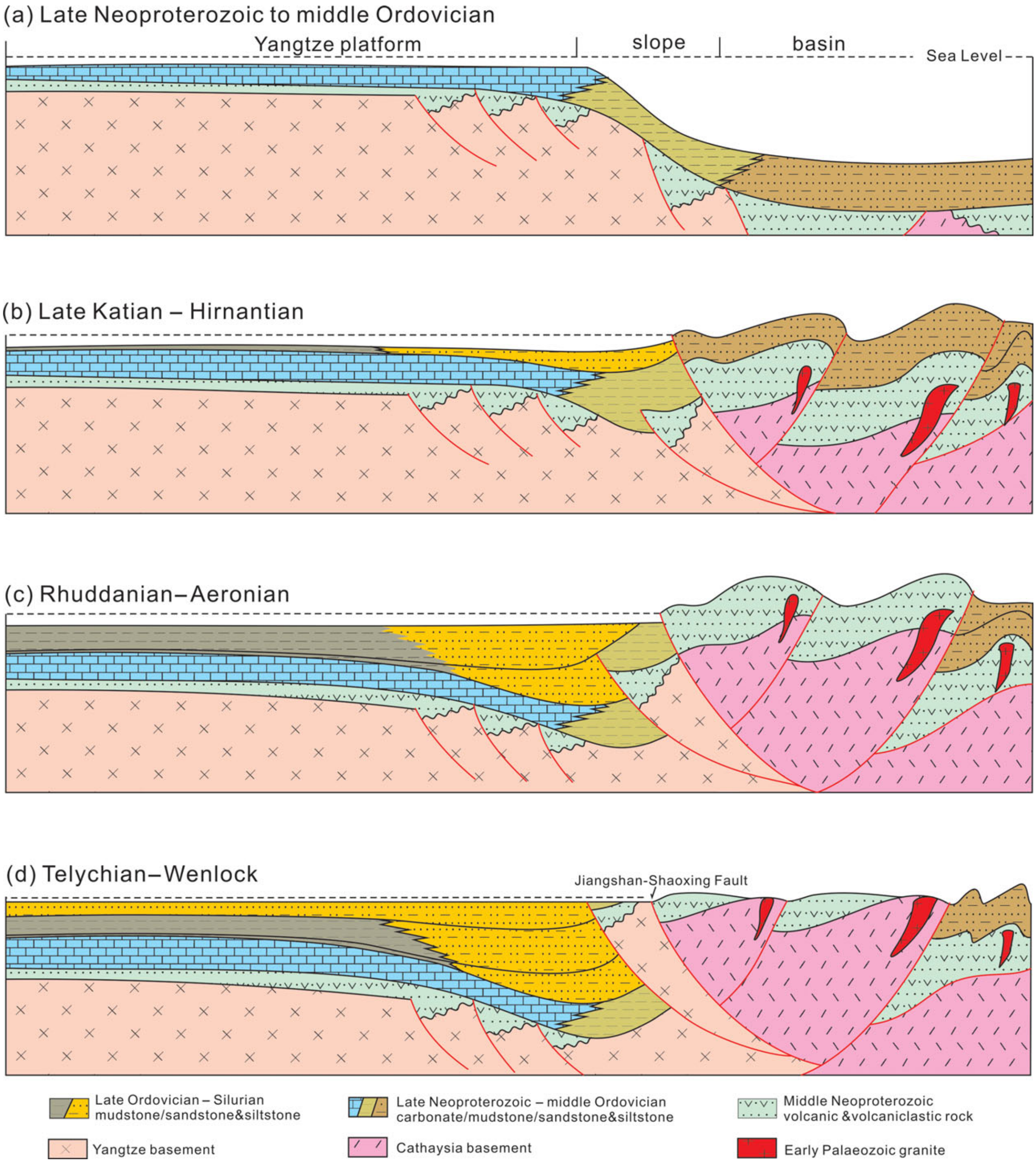

Figure 9. Schematic reconstruction of the filling history of the Lower Yangtze foreland basin and the uplifting and unroofing process of the Wuyi–Yunkai orogenic belt. (a) During the late Neoproterozoic to middle Ordovician, the study area was in a passive margin setting; (b) during the late Ordovician, the detritus derived from the recycled pre-orogenic rocks formed a wedge in the foreland basin; (c) during the Rhuddanian to Aeronian, massive subsidence occurred in the foreland basin and the middle Neoproterozoic rocks provided a large amount of detritus; (d) during the Telychian to Wenlock, the foreland basin was overfilled, and the synorogenic magmatic rocks were exhumed to provide detritus.

source, and implies that the orogenic uplift may have formed a topographic barrier to prevent sediment input from the recycled source. The presence of a component of synorogenic detritus in the Aeronian sample reflects that the magmatic and the metamorphic rocks formed during the Wuyi–Yunkai orogeny had been exposed to serve as a source since the Aeronian.

During Telychian (late Llandovery) to Wenlock times the foreland basin was filled with shallowing-upwards deposits (Fig. 9d), as revealed by the widespread occurrence of red sandstone (Chen *et al.* 1988; Rong *et al.* 2003). This fact implies that the sediment supply had outpaced the tectonic subsidence. The three samples from the upper Llandovery to Wenlock strata contain a major component of detrital zircons in the range of 880–740 Ma, suggesting that significant detritus from the middle Neoproterozoic volcanic rocks probably persisted. The reappearance of Grenville-age

https://doi.org/10.1017/S0016756812000969 Published online by Cambridge University Press

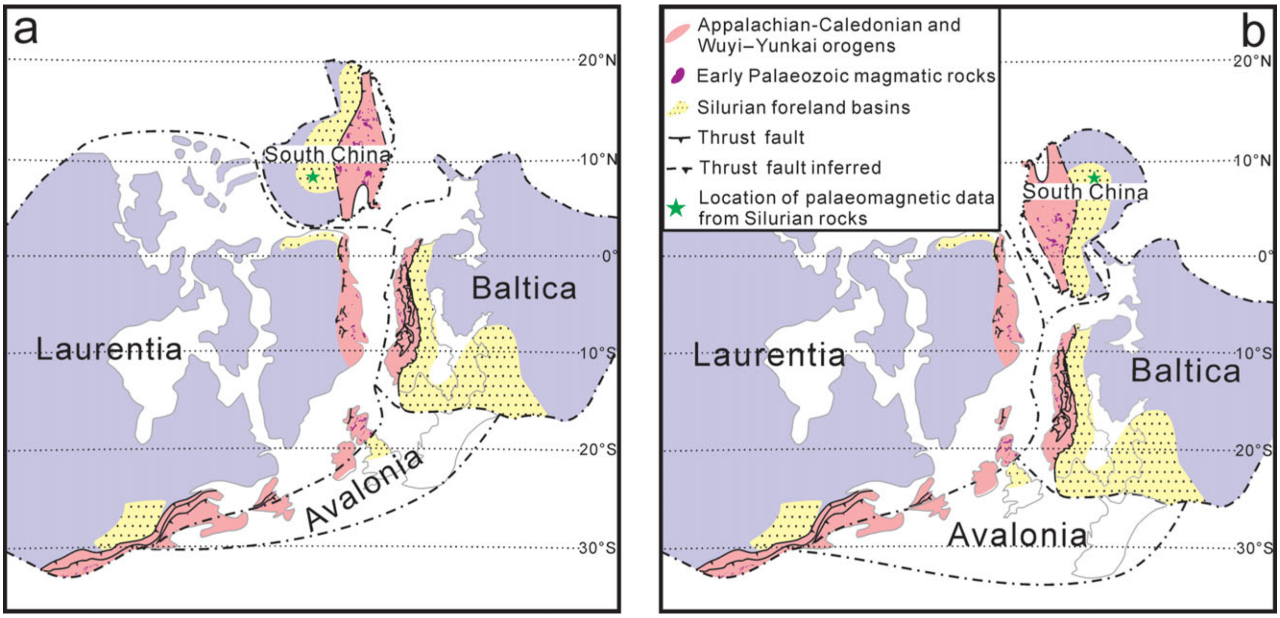

Figure 10. Two possible positions of the South China block at *c.* 425 Ma, based on tectonic features and palaeolatitude (Huang, Opdyke & Zhu, 2000): (a) modified from Cocks & Torsvik (2005); (b) after Dewey & Strachan (2003). Tectonic framework of the Appalachian and Caledonian orogens and foreland basins from Kneller (1991), Nikishin *et al.* (1996), Higgins & Leslie (2000), Ettensohn (2004), Gee *et al.* (2008), Oliver, Wilde & Wan (2008), Bingen & Solli (2009) and Hibbard, van Staal & Rankin (2010).

zircons may imply that detritus recycled from the pre-orogenic rocks was not significantly affected by the topographic barrier. An alternative explanation is that the detritus was derived directly from the first-cycle source area on the southeastern margin of the Yangtze block. A significant number of detrital zircons ranging in age from 460 to 425 Ma correspond well with the age of the Wuyi–Yunkai orogen, and suggest that the synorogenic magmatic and metamorphic rocks were progressively exhumed to provide detritus.

The age of the youngest zircons from the upper unit of the Silurian strata provides a depositional age. From these data, the development of the foreland basin is inferred to last until *c.* 425 Ma. The initiation of the foreland basin is constrained by the biostratigraphic data, which gave an age of *c.* 448 Ma (Rong *et al.* 2010). Therefore, the Lower Yangtze foreland basin is supposed to have developed from *c.* 448 to 425 Ma. As the formation of the foreland basin has a close relationship with the thrust loading, this age range provides a time constraint on the deformation and uplift of the Wuyi–Yunkai orogeny.

5.c. Tectonic implications

There is still no consensus on the tectonic setting and geodynamic driving force for the early Palaeozoic orogeny in South China. Some authors regard the Wuyi–Yunkai orogen as a collisional orogen, which was formed owing to arc–continent collision (Guo *et al.* 1989; Yang *et al.* 1995; Ma, 2006) or closure of a small oceanic basin between the Yangtze and Cathaysia blocks (Liu & Xu, 1994). This collisional orogenic model was questioned because evidence of an active continental margin is absent in South China (Hu *et al.* 1992; Faure *et al.* 2009; Li *et al.* 2010; Charvet *et al.* 2010). Other workers (Ren & Chen, 1989; Wang, Y. J. *et al.* 2007; Faure *et al.* 2009; Li *et al.* 2010) have proposed intracontinental orogenic or intraplate models, based on the lack of early Palaeozoic ophiolites, a magmatic arc, subduction complexes or paired metamorphic belts in the orogenic belt that are indicative of an active continental margin. However, the priming process for the intracontinental orogen is not clear. Faure *et al.* (2009) and Charvet *et al.* (2010) considered that the orogen was caused by intracontinental deformation, while other authors (e.g. Li, 1998; Li & Powell, 2001; Wang *et al.* 2010) supposed that the orogeny was the result of interactions between the Cathaysia block margin and the Australian–Indian margin of Gondwanaland. However, this assumption is challenged by the fact that South China was likely separated from Gondwana during the late Ordovician and early Silurian, as indicated by great differences in shelly faunas and lithofacies between the two regions (Cocks & Torsvik, 2002; Rong *et al.* 2003). On the contrary, the provenance studies of the Cambrian to Ordovician deposits suggest that South China seems to have a Laurentian affinity instead of Gondwanan (Wu *et al.* 2010). As the Wuyi–Yunkai orogeny was mostly synchronous with the late stages of the Caledonian orogeny (McKerrow, MacNiocaill & Dewey, 2000), we compare the geological features of the Wuyi–Yunkai orogen with the Appalachian–Caledonide orogen and find they share some similarities. Both orogens are characterized by intense deformation, widespread magmatism and metamorphism and accompanied by foreland basins (e.g. Kneller, 1991; Nikishin *et al.*

https://doi.org/10.1017/S0016756812000969 Published online by Cambridge University Press

1996; Higgins & Leslie, 2000; Ettensohn, 2004; Gee *et al*. 2008; Gilotti, Jones & Elvevold, 2008; Oliver, Wilde & Wan, 2008; Bingen & Solli, 2009; Hibbard, van Staal & Rankin, 2010; Cocks & Torsvik, 2011). Given these facts, we tentatively infer that there may be a possible link between the two orogens. The available palaeomagnetic data from the Silurian sandstones in the southwestern Yangtze region suggest that the sampling area was located in low latitudes (8.3° ± 4.0), and most likely in the northern hemisphere (Huang, Opdyke & Zhu, 2000). Based on the palaeomagnetic data and geological constraints, two possible positions of the South China block at *c*. 425 Ma are proposed. One is that it was situated to the north of Laurentia (Fig. 10a), which had collided with Baltica and Avalonia to form Laurussia (Cocks & Torsvik, 2005, 2011). The alternative is that it was located to the north of Baltica (Fig. 10b), which was obliquely colliding with Laurentia (Dewey & Strachan, 2003). To test these hypotheses, more early Palaeozoic palaeomagnetic data are needed, which are rather scarce in the South China block, and detailed work should be carried out on the tectonics and evolution of the Wuyi–Yunkai orogen, which are still not well constrained.

6. Conclusion

(1) The zircons from the upper Ordovician and Silurian strata show a broad range in ages, from a maximum of 3468 Ma to as young as 425 Ma, with clusters at 2500–2400 Ma, 2000–1700 Ma, 1200–950 Ma, 880–740 Ma and 460–425 Ma.

(2) The overall age range of the detritus is consistent with derivation from the Wuyi–Yunkai orogen. Most of the zircons older than 900 Ma were likely recycled from the pre-orogenic strata with minor contributions from Grenville-age rocks. The zircons with ages between 880 and 740 Ma were derived from the middle Neoproterozoic volcanic rocks and the recycled strata. The zircons having ages of 460–425 Ma were shed from the synorogenic magmatic and metamorphic rocks.

(3) The temporal trends in zircon age patterns provide new insights into the unroofing evolution of the Wuyi–Yunkai orogen. During the late Ordovician, the pre-orogenic strata were uplifted and eroded. In the early Llandovery, the middle Neoproterozoic volcanic rocks were extensively eroded. From the late Llandovery onwards, the synorogenic magmatic and metamorphic rocks were exposed to denudation.

(4) The youngest zircon age with available biostratigraphic data from the synorogenic deposits indicates that the Lower Yangtze foreland basin formation took place during 448–425 Ma.

Acknowledgements. We would like to express our gratitude to Professor Jacques Charvet and two anonymous reviewers for their careful reviewing and constructive suggestions. Thanks to Jinhai Yu for operation of and assistance with LA-ICP-MS in the State Key Laboratory for Mineral Deposits Research at Nanjing University. We are also grateful to Yongxiang Li for his assistance in improving the manuscript. This study is funded by the National Basic Research Program of China (973 Program) (2012CB214703), National S&T Major Project of China (2011ZX05009-001 and 2011ZX05003-001) and the Ph.D. Programmes Foundation of the Ministry of Education of China (20090091110020).

References

ABGMR (ANHUI BUREAU OF GEOLOGY AND MINERAL RESOURCES). 1997. *Multiple Classification of Stratigraphy of China (34), Stratigraphy (Lithostratigraphic) of Anhui Province*. Wuhan: China University of Geosciences Press, 721 pp. (in Chinese with English abstract).

ANDERSEN, T. 2002. Correction of common lead in U–Pb analyses that do not report ^{204}Pb. *Chemical Geology* **192**, 59–79.

BINGEN, B. & SOLLI, A. 2009. Geochronology of magmatism in the Caledonian and Sveconorwegian belts of Baltica: synopsis for detrital zircon provenance studies. *Norwegian Journal of Geology* **89**, 267–90.

BRADLEY, D. C. 2008. Passive margins through earth history. *Earth-Science Reviews* **91**, 1–26.

CAWOOD, P. A., NEMCHIN, A. A., LEVERENZ, A., SAEED, A. & BALLANCE, P. F. 1999. U/Pb dating of detrital zircons: implications for the provenance record of Gondwana margin terranes. *Geological Society of America Bulletin* **111**, 1107–19.

CAWOOD, P. A., NEMCHIN, A. A., STRACHAN, R. A., PRAVE, T. & RABBENDAM, M. 2007. Sedimentary basin and detrital zircon record along East Laurentia and Baltica during assembly and breakup of Rodinia. *Journal of the Geological Society, London* **164**, 257–75.

CHARVET, J., SHU, L. S., FAURE, M., CHOULET, F., WANG, B., LU, H. F. & BRETON, N. L. 2010. Structural development of the Lower Palaeozoic belt of South China: genesis of an intracontinental orogen. *Journal of Asian Earth Sciences* **39**, 309–30.

CHARVET, J., SHU, L. S., SHI, Y. S., GUO, L. Z. & FAURE, M. 1996. The building of South China: collision of Yangtze and Cathaysia blocks, problems and tentative answers. *Journal of Southeast Asian Earth Sciences* **13**, 223–35.

CHEN, X., CHEN, T. E., ZOU, X. P., QIU, J. Y., NI, Y. N. & YANG, X. C. 1988. Ordovician of the Lower Yangtze in Jiangsu region. In *Sinian-Triassic Biostratigraphy of the Lower Yangtze Peneplatform in Jiangsu Region* (eds Geological Sciences Institute of Jiangsu Petroleum Bureau and Nanjing Institute of Geology and Palaeontology), pp. 81–126. Nanjing: Nanjing University Press (in Chinese).

CHEN, X. & RONG, J. Y. 1996. *Telychian (Llandovery) of the Yangtze Region and its correlation with British Isles*. Beijing: Science Press, 162 pp. (in Chinese with English abstract).

CHEN, X., RONG, J. Y., LI, Y. & BOUCOT, A. J. 2004. Facies patterns and geography of the Yangtze region, South China, through the Ordovician and Silurian transition. *Palaeogeography, Palaeoclimatology, Palaeoecology* **204**, 353–72.

CHEN, X., RONG, J. Y., MITCHELL, C. E., HARPER, D. A. T., FAN, J. X., ZHAN, R. B., ZHANG, Y. D., LI, R. Y. & WANG, Y. 2000. Late Ordovician to earliest Silurian graptolite and brachiopod biozonation from the Yangtze region, South China with a global correlation. *Geological Magazine* **137**, 623–50.

CHEN, X., ROWLEY, D., RONG, J. Y., ZHANG, J., ZHANG, Y. D. & ZHAN, R. B. 1997. Late Precambrian through Early Palaeozoic stratigraphic and tectonic evolution of the Nanling Region, Hunan Province, South China. *International Geology Review* **39**, 469–78.

Chen, X., Zhang, Y. D., Fan, J. X., Cheng, J. F. & Li, Q. J. 2010. Ordovician graptolite-bearing strata in southern Jiangxi with a special reference to the Kwangsian Orogeny. *Science China Earth Sciences* **53**, 1602–10.

Chen, X., Zhou, Z. Y. & Fan, J. X. 2010. Ordovician palaeogeography and tectonics of the major palaeoplates of China. In *The Ordovician Earth System* (eds S. C. Finney & W. B. N. Berry), pp. 85–104. Geological Society of America, Special Papers no. 466.

Cocks, L. R. M. & Torsvik, T. H. 2002. Earth geography from 500 to 400 million years ago: a faunal and palaeomagnetic review. *Journal of the Geological Society, London* **159**, 631–44.

Cocks, L. R. M. & Torsvik, T. H. 2005. Baltica from the late Precambrian to mid-Palaeozoic times: the gain and loss of a terrane's identity. *Earth-Science Reviews* **72**, 39–66.

Cocks, L. R. M. & Torsvik, T. H. 2011. The Palaeozoic geography of Laurentia and western Laurussia: a stable craton with mobile margins. *Earth-Science Reviews* **106**, 1–51.

Dewey, J. F. & Strachan, R. A. 2003. Changing Silurian-Devonian relative plate motion in the Caledonides: sinistral transpression to sinistral transtension. *Journal of the Geological Society, London* **160**, 219–29.

Ettensohn, F. R. 2004. Modeling the nature and development of major Paleozoic clastic wedges in the Appalachian Basin, USA. *Journal of Geodynamics* **37**, 657–81.

Faure, M., Shu, L. S., Wang, B., Charvet, J., Choulet, F. & Monie, P. 2009. Intracontinental subduction: a possible mechanism for the Early Palaeozoic Orogen of SE China. *Terra Nova* **21**, 360–8.

Gee, D. G., Fossen, H., Henriksen, N. & Higgins, A. K. 2008. From the Early Paleozoic platforms of Baltica and Laurentia to the Caledonide Orogen of Scandinavian and Greenland. *Episodes* **31**, 44–51.

Gilotti, J. A., Jones, K. A. & Elvevold, S. 2008. Caledonian metamorphic patterns in Greenland. In *The Greenland Caledonides: Evolution of the Northeast Margin of Laurentia* (eds A. K. Higgins, J. A. Gilotti & M. P. Smith), pp. 201–5. Geological Society of America, Memoir no. 202.

Guo, L. Z., Shi, Y. S., Lu, H. F., Ma, R. S., Dong, H. G. & Yang, S. F. 1989. The pre-Devonian tectonic patterns and evolution of South China. *Journal of SE Asian Earth Sciences* **3**, 87–93.

Hibbard, J. P., van Staal, C. R. & Rankin, D. W. 2010. Comparative analysis of the geological evolution of the northern and southern Appalachian orogen: Late Ordovician-Permian. In *From Rodinia to Pangea: The Lithotectonic Record of the Appalachian Region* (eds R. P. Tello, M. J. Bartholomew, J. P. Hibbard & P. M. Karabinos), pp. 51–69. Geological Society of America, Memoir no. 206.

Higgins, A. K. & Leslie, A. G. 2000. Restoring thrusting in the East Greenland Caledonides. *Geology* **28**, 1019–22.

Hu, X. J., Xu, J. K., Tong, C. X., Chen, C. H. & Ye, G. K. 1992. Geological features and tectonic evolution of the middle Proterozoic Longquan Group in Southern Zhejiang. *Regional Geology of China* **1**, 20–30 (in Chinese with English abstract).

Huang, K., Opdyke, N. & Zhu, R. X. 2000. Further paleomagnetic results from the Silurian of the Yangtze Block and their implications. *Earth and Planetary Science Letters* **175**, 191–202

Jackson, S. E., Pearson, N. J., Griffin, W. L. & Belousova, E. A. 2004. The application of laser ablation-inductively coupled plasma-mass spectrometry to in situ U–Pb zircon geochronology. *Chemical Geology* **211**, 47–69.

JBGMR (Jiangsu Bureau of Geology and Mineral Resources). 1984. *Regional Geology of Jiangsu Province and Shanghai City*. Beijing: Geological Publishing House, 857 pp. (in Chinese with English abstract).

Jiang, G., Kennedy, M. J. & Christie-Blick, N. 2003. Stable isotopic evidence for methane seeps in Neoproterozoic postglacial cap carbonates. *Nature* **426**, 822–26.

Jiang, G., Sohl, L. E. & Christie-Blick, N. 2003. Neoproterozoic stratigraphic comparison of the Lesser Himalaya (India) and Yangtze block (south China): paleogeographic implications. *Geology* **31**, 917–20.

Kneller, B. C. 1991. A foreland basin on the southern margin of Iapetus. *Geology* **148**, 207–10.

Li, L. M., Sun, M., Wang, Y. J., Xing, G. F., Zhao, G. C., Lin, S. F., Xia, X. P., Chan, L. S., Zhang, F. F. & Wong, J. 2011. U–Pb and Hf isotopic study of zircons from migmatised amphibolites in the Cathaysia Block: implications for the early Paleozoic peak tectonothermal event in Southeastern China. *Gondwana Research* **19**, 191–201.

Li, W. X., Li, X. H. & Li, Z. X. 2005. Neoproterozoic bimodal magmatism in the Cathaysia Block of South China and its tectonic significance. *Precambrian Research* **136**, 51–66.

Li, W. X., Li, X. H., Li, Z. X. & Lou, F. S. 2008. Obduction-type granites within the NE Jiangxi ophiolite: implications for the final amalgamation between the Yangtze and Cathaysia blocks. *Gondwana Research* **13**, 288–301.

Li, X. H., Li, W. X., Li, Z. X. & Liu, Y. 2008. 850–790 Ma bimodal volcanic and intrusive rocks in northern Zhejiang, South China: a major episode of continental rift magmatism during the breakup of Rodinia. *Lithos* **102**, 341–57.

Li, X. H., Zhou, G., Zhao, J., Fanning, C. M. & Compston, W. 1994. SHRIMP ion microprobe zircon U–Pb age of the NE Jiangxi ophiolite and its tectonic implications. *Geochimica* **23**, 125–31 (in Chinese with English abstract).

Li, Z. X. 1998. Tectonic history of the major East Asian lithospheric blocks since the mid-Proterozoic: a synthesis. In *Mantle Dynamics and Plate Interactions in East Asia* (eds M. J. Flower, S. L. Chung, C. H. Lo & T. Y. Lee), pp. 221–43. American Geophysical Union Geodynamics Series no. 27. Washington, DC, USA.

Li, Z. X., Li, X. H., Kinny, P. D. & Wang, J. 1999. The breakup of Rodinia: did it start with a mantle plume beneath South China? *Earth and Planetary Science Letters* **173**, 171–81.

Li, Z. X., Li, X. H., Kinny, P. D., Wang, J., Zhang, S. & Zhou, H. 2003. Geochronology of Neoproterozoic syn-rift magmatism in the Yangtze Craton, South China and correlations with other continents: evidence for a mantle superplume that broke up Rodinia. *Precambrian Research* **122**, 85–109.

Li, Z. X., Li, X. H., Wartho, J. A., Clark, C., Li, W. X., Zhang, C. L. & Bao, C. 2010. Magmatic and metamorphic events during the early Palaeozoic Wuyi-Yunkai orogeny, southeastern South China: new age constraints and pressure–temperature conditions. *Geological Society of America Bulletin* **122**, 772–93.

https://doi.org/10.1017/S0016756812000969 Published online by Cambridge University Press

Li, Z. X., Li, X. H., Zhou, H. W. & Kinny, P. D. 2002. Grenvillian continental collision in South China: new SHRIMP U–Pb zircon results and implications for the configuration of Rodinia. *Geology* **30**, 163–6.

Li, Z. X. & Powell, C. M. 2001. An outline of the palaeogeographic evolution of the Australasian region since the beginning of the Neoproterozoic. *Earth-Science Reviews* **53**, 237–77.

Liu, B. J. & Xu, X. S. 1994. *Atlas of Lithofacies and Palaeogeography of South China (Sinian to Triassic)*. Beijing: Science Press, 188 pp. (in Chinese).

Liu, R., Zhou, H. W., Zhang, L., Zhong, Z. Q., Zeng, W., Xiang, H., Jin, S., Lu, X. Q. & Li, C. Z. 2009. Paleoproterozoic reworking of ancient crust in the Cathaysia Block, South China: evidence from zircon trace elements, U–Pb and Lu–Hf isotopes. *Chinese Science Bulletin* **54**, 1543–54.

Liu, R., Zhou, H. W., Zhang, L., Zhong, Z. Q., Zeng, W., Xiang, H., Jin, S., Lu, X. Q. & Li, C. Z. 2010. Zircon U–Pb ages and Hf isotope compositions of the Mayuan migmatite complex, NW Fujian Province, Southeast China: constraints on the timing and nature of a regional tectonothermal event associated with the Caledonian orogeny. *Lithos* **119**, 163–80.

Ma, R. S. 2006. New thought about the tectonic evolution of the South China: with discussion on several problems of the Cathaysian Oldland. *Geological Journal of China Universities* **12**, 448–56 (in Chinese with English abstract).

McKerrow, W. S., MacNiocall, C. & Dewey, J. F. 2000. The Caledonian Orogeny redefined. *Journal of the Geological Society, London* **157**, 1149–54.

Mu, E. Z., Boucot, A. J., Chen, X. & Rong, J. Y. 1986. *Correlation of the Silurian Rocks of China (A Part of the Silurian Correlation for East Asia)*. Geological Society of America Special Paper no. 202, 80 pp.

Nikishin, A. M., Ziegler, P. A., Stephenson, R. A., Cloetingh, S. A. P. L., Furne, A. V., Fokin, P. A., Ershov, A. V., Bolotov, S. N., Korotaev, M. V., Alekseev, A. S., Gorbachev, V. I., Shipilov, E. V., Lankreijer, A., Bembinova, E. Y. & Shalimov, I. V. 1996. Late Precambrian to Triassic history of the East European Craton: dynamics of sedimentary basin evolution. *Tectonophysics* **268**, 23–63.

Oliver, G. J. H., Wilde, S. A. & Wan, Y. S. 2008. Geochronology and geodynamics of Scottish granitoids from the late Neoproterozoic break-up of Rodinia to Palaeozoic collision. *Journal of Geology Society, London* **165**, 661–74.

Qiu, Y. M., Gao, S., McNaughton, N. J., Groves, D. I. & Ling, W. L. 2000. First evidence of >3.2 Ga continental crust in the Yangtze Craton of south China and its implications for Archean crustal evolution and Phanerozoic tectonics. *Geology* **28**, 11–4.

Ren, J. S. & Chen, T. Y. 1989. Tectonic evolution of the continental lithosphere in eastern China and adjacent areas. *Journal of Southeast Asian Earth Sciences* **3**, 17–27.

Ren, J. S. 1991. On the geotectonics of southern China. *Acta Geologica Sinica* **4**, 111–30.

Rong, J. Y. & Chen, X. 1987. Faunal differentiation, biofacies and lithofacies pattern of late Ordovician (Ashgillian) in South China. *Acta Palaeontologica Sinica* **26**, 507–35.

Rong, J. Y., Chen, X., Zheng, S. Y., Ni, Y. N., Zhan, R. B., Chen, T. E., Fu, L. P., Li, R. Y. & Fan, J. X. 2003. Silurian palaeogeography of China. In *Silurian Lands and Seas, Palaeogeography Outside of Laurentia* (eds E. Landing & M. E. Johnson), pp. 243–98. New York State Museum Bulletin no. 493.

Rong, J. Y., Zhan, R. B., Xu, H. G., Huang, B. & Yu, G. H. 2010. Expansion of the Cathaysian Oldland through the Ordovician–Silurian transition: emerging evidence and possible dynamics. *Science China Earth Sciences* **53**, 1–17.

Shu, L. S., Faure, M., Yu, J. H. & Jahn, B. M. 2011. Geochronological and geochemical features of the Cathaysia block (South China): new evidence for the Neoproterozoic breakup of Rodinia. *Precambrian Research* **187**, 263–76.

Vernhet, E., Heubeck, C., Zhu, M. Y. & Zhang, J. M. 2006. Large-scale slope instability at the southern margin of the Ediacaran Yangtze Platform (Hunan province, central China). *Precambrian Research* **148**, 32–44.

Wan, Y. S., Liu, D. Y., Wilde, S. A., Cao, J. J., Chen, B., Dong, C. Y., Song, B. & Du, L. L. 2010. Evolution of the Yunkai Terrane, South China: evidence from SHRIMP zircon U–Pb dating, geochemistry and Nd isotope. *Journal of Asian Earth Sciences* **37**, 140–53.

Wan, Y. S., Liu, D., Xu, M., Zhuang, J., Song, B., Shi, Y. & Du, L. 2007. SHRIMP U–Pb zircon geochronology and geochemistry of metavolcanic and metasedimentary rocks in NW Fujian, Cathaysian block, China: tectonic implications and the need to redefine lithostratigraphic units. *Gondwana Research* **12**, 166–83.

Wang, J. & Li, Z. X. 2003. History of Neoproterozoic rift basins in South China: implications for Rodinia break-up. *Precambrian Research* **122**, 141–58.

Wang, X. L., Zhou, J. C., Qiu, J. S. & Gao, J. F. 2004. Geochemistry of the Meso- to Neoproterozoic basic-acid rocks from Hunan Province, South China: implications for the evolution of the western Jiangnan orogen. *Precambrian Research* **135**, 79–103.

Wang, X. L., Zhou, J. C., Griffin, W. L., Wang, R. C., Qiu, J. S., O'Reilly, S. Y., Xu, X. S., Liu, X. M. & Zhang, G. L. 2007. Detrital zircon geochronology of Precambrian basement sequences in the Jiangnan orogen: dating the assembly of the Yangtze and Cathaysia Blocks. *Precambrian Research* **159**, 117–31.

Wang, X. L., Zhou, J. C., Qiu, J. S., Zhang, W. L., Liu, X. M. & Zhang, G. L. 2006. LA-ICP-MS zircon geochronology of the Neoproterozoic igneous rocks from Northern Guangxi, South China: implications for tectonic evolution. *Precambrian Research* **145**, 111–30.

Wang, Y. J., Fan, W. M., Zhao, G. C., Ji, S. C. & Peng, T. P. 2007. Zircon U–Pb geochronology of gneissic rocks in the Yunkai massif and its implications on the Caledonian event in the South China Block. *Gondwana Research* **12**, 404–16.

Wang, Y. J., Zhang, A. M., Fan, W. M., Zhao, G. C., Zhang, G. W., Zhang, Y. Z., Zhang, F. F. & Li, S. Z. 2011. Kwangsian crustal anatexis within the eastern South China Block: geochemical, zircon U–Pb geochronological and Hf isotopic fingerprints from the gneissoid granites of Wugong and Wuyi–Yunkai Domains. *Lithos* **127**, 239–60.

Wang, Y. J., Zheng, F. F., Fan, W. M., Zhang, G. W., Chen, S. Y., Cawood, P. A. & Zhang, A. M. 2010. Tectonic setting of the South China Block in the early Palaeozoic: resolving intracontinental and ocean closure models from detrital zircon U–Pb geochronology. *Tectonics* **29**, 1–16.

Wu, L., Jia, D., Li, H. B., Deng, F. & Li, Y. Q. 2010. Provenance of detrital zircons from the late Neoproterozoic to

https://doi.org/10.1017/S0016756812000969 Published online by Cambridge University Press

Ordovician sandstones of South China: implications for its continental affinity. *Geological Magazine* **176**, 974–80.

XIA, B. D. & LU, H. B. 1990. A study on a buried fossil orogenic belt. *Acta Sedimentologica Sinica* **8**, 1–8 (in Chinese with English abstract).

XU, K. Q., LIU, Y. J., YU, S. J., WANG, H. N. & WEI, X. Z. 1960. The discovery of the Caledonian granite in South Jiangxi Province. *Geological Review* **20**, 112–4 (in Chinese).

XU, X. B., ZHANG, Y. Q., SHU, L. S. & JIA, D. 2011. La-ICP-MS U–Pb and $^{40}Ar/^{39}Ar$ geochronology of the sheared metamorphic rocks in the Wuyishan: constraints on the timing of Early Palaeozoic and Early Mesozoic tectonothermal events in SE China. *Tectonophysics* **501**, 71–86.

YANG, S. F., CHEN, H. L., WU, G. H. & DONG, C. W. 1995. Discovery of early Paleozoic island-arc volcanic rocks in north part of Fujian Province and the significance for tectonic study. *Scientia Geologica Sinica* **30**, 105–16 (in Chinese with English abstract).

YANG, D. S., LI, X. H., LI, W. X., LIANG, X. H., LONG, W. G. & XIONG, X. L. 2010. U–Pb and ^{40}Ar–^{39}Ar geochronology of the Baiyunshan gneiss (central Guangdong, south China): constraints on the timing of early Palaeozoic and Mesozoic tectonothermal events in the Wuyun (Wuyi-Yunkai) Orogen. *Geological magazine* **147**, 481–96.

YAO, J. L., SHU, L. S. & SANTOSH, M. 2011. Detrital zircon U–Pb geochronology, Hf-isotopes and geochemistry – new clues for the Precambrian crustal evolution of Cathaysia Block, South China. *Gondwana Research* **20**, 553–67.

YE, M. F., LI, X. H., LI, W. X., LIU, Y. & LI, Z. X. 2007. SHRIMP zircon U-Pb geochronological and whole-rock geochemical evidence for an early Neoproterozoic Sibaoan magmatic arc along the southeastern margin of the Yangtze Block. *Gondwana Research* **12**, 144–56.

YU, J. H., O'REILLY, S. Y., WANG, L. J., GRIFFIN, W. L., ZHANG, M., WANG, R. C., JIANG, S. Y. & SHU, L. S. 2008. Where was South China in the Rodinia supercontinent? Evidence from U–Pb geochronology and Hf isotopes of detrital zircons. *Precambrian Research* **164**, 1–15.

YU, J. H., WANG, L. J., GRIFFIN, W. L., O'REILLY, S. Y., ZHANG, M., LI, C. Z. & SHU, L. S. 2009. A Paleoproterozoic orogeny recorded in a long-lived cratonic remnant (Wuyishan terrane), eastern Cathaysia Block, China. *Precambrian Research* **174**, 347–63.

ZBGMR (ZHEJIANG BUREAU OF GEOLOGY AND MINERAL RESOURCES). 1965. *Regional Geological Survey Report (Jiande area, 1:200000)*, 162 pp. (in Chinese).

ZBGMR (ZHEJIANG BUREAU OF GEOLOGY AND MINERAL RESOURCES). 1989. *Regional Geology of Zhejiang Province*. Beijing: Geological Publishing House, 688 pp. (in Chinese with English abstract).

ZHANG, Z. M., LIOU, J. G. & COLEMAN, R. G. 1984. An outline of the plate tectonics of China. *Geological Society of America Bulletin* **95**, 295–312.

ZHAO, G. & CAWOOD, P. 1999. Tectonothermal evolution of the Mayuan assemblage in the Cathaysia Block: implications for Neoproterozoic collision-related assembly of the South China Craton. *American Journal of Science* **299**, 309–39.

ZHENG, Y. F., WU, R. X., WU, Y. B., ZHANG, S. B., YUAN, H. L. & WU, F. Y. 2008. Rift melting of juvenile arc-derived crust: geochemical evidence from Neoproterozoic volcanic and granitic rocks in the Jiangnan Orogen, South China. *Precambrian Research* **163**, 351–83.

ZHOU, C. M., TUCKER, R., XIAO, S., PENG, Z., YUAN, X. & CHEN, Z. 2004. New constraints on the ages of Neoproterozoic glaciations in south China. *Geology* **32**, 437–40.

ZHOU, M. F., YAN, D. P., KENNEDY, A. K., LI, Y. Q. & DING, J. 2002. SHRIMP U-Pb zircon geochronological and geochemical evidence for Neoproterozoic arc-magmatism along the western margin of the Yangtze block, South China. *Earth and Planetary Science Letters* **196**, 51–67.